Modeling Production Rate in Rock Excavation Operations by Predicting Rock Properties Using Neural Networks

Pedro Pablo Vasquez-Coronado[1] and Eugene Ben-Awuah[2]

[1,2] Bharti School of Engineering and Computation, Laurentian University, Sudbury, Ontario, Canada

ABSTRACT

In mining operations, the production rate is significantly influenced by the physical properties of the rock, such as density, compressive strength, and abrasiveness. These properties directly determine the extent of fracturing and extracting the rock, which in turn affects the overall production rate. To illustrate the importance of how to measure these rock features, this study used neural network models to estimate two key rock properties: density and point load strength. Experimental data was collected from rock samples with varying compositions and divided into separate sets for training and testing the models. After preparing the data, neural network models with several dense layers and non-linear functions were built and trained, incorporating techniques to prevent overfitting. The models performed well in predicting density and point load strength, achieving low error rates when evaluated on the test sets. By integrating predictions of these rock properties into production rate models, it became possible to quantify how factors like density and strength influence excavation productivity. This allows for optimization by relating controllable parameters to the target production rate while considering the site-specific rock characteristics. This study demonstrates how integrating machine learning techniques, such as neural networks, can improve predictive models used in rock excavation operations.

1. Introduction

In open pit mining, excavation and hauling activities are decisive for productivity and costs. This study aims to create a model to predict haulage costs in blasting operations, considering different factors that affect the excavation process.

The research predicts a shovel's production rate. This is calculated by multiplying an ideal maximum productivity rate by operational efficiency [28] . To calculate the production rate, the research employs two deep learning libraries TensorFlow and Keras [23] . These libraries allow the creation, training, and deployment of deep neural network models. Two predictive models were created: one to estimate rock density based on aluminum oxide (Al_2O_3) content, and the other to predict the point load strength index ($I_s(50)$) using both density and Al_2O_3 content.

The rock density prediction model is implemented using Al_2O_3 grade. To predict the values of $I_s(50)$, the model uses a combination of density and Al_2O_3 dataset to predict $I_s(50)$. Using the predicted values, the model can estimate haulage rates.

ISBN: 978-1-55195-520-9

Theoretical models and machine learning prediction are used in this study to enhance the analysis and prediction of the haulage rates in open pit operations. Specifically, the objective of the research is to contribute to the enhancement of mining rock excavation processes taking into consideration rock properties such as density and point load strength. Thus, this will enhance operational effectiveness and efficiency in resource utilization and equipment allocation.

2. Literature Review

In this section, recent developments in production rate modeling, variables influencing the excavation process, the prediction of rock properties, and the use of machine learning techniques in the mining sector are all covered.

2.1. Current Approaches to Production Rate Modeling in Open Pit Mining

Researchers have experimented with a variety of techniques, such as computer simulations that mimic the production of ore by employing models like Petri nets. These techniques give better estimates than older methods [17] . These models have been further enhanced with agent-based approaches to evaluate production targets and track fuel consumption by haul trucks [22].

Comprehensive models that combine pit design and production planning have been developed to maintain smooth processing plant operations and steady ore feed [6] . Researchers have also utilized simulations and mathematical techniques to optimize production schedules and maximize cash flow throughout the mine's life [7, 25].

Mining production capacity is limited by the processing plant's capacity and the average ore grade [15] Studies on cut-off grade optimization have revealed that balancing mining and processing capacities is crucial for maximizing production.

2.2. Factors Affecting Excavation Processes

Several factors affect mining operations, including safety, environment, and other related activities. Lukashuk et al. [18] looked at how to control excavators in open pit mines. The authors found that the mechanics of lifting and thrusting to work together were key to achieving good digging. An experiment used a computer program to test the operating conditions of an excavator's bucket movement along a planned path, resulting in a digging algorithm and control functions based on the bucket's position, which can be used to design control systems for open-pit excavators.

Zhang et al. [35] showed the importance of keeping slopes stable which helps to ensure safety in open pit operations. Having knowledge about slope stability and soil properties helps prevent rock falls in open pit mines. Cao et al. [5] added that knowing the state of in situ rock formations assists in understanding the effect of blasting on slope stability.

Kolapo et al. [16] reviewed case studies of slope failures in mining operations, explained failure modes and influencing factors, and highlighted the importance of monitoring and evaluating slope stability. The authors proposed the integration of analytical methods with artificial intelligence to improve prediction accuracy and security.

2.3. Methods Used for Rock Property Prediction

Predicting rock properties is extremely important for various engineering and construction projects, most especially in mining. The key characteristics that indicate rock mechanical strength and behavior are density and point load index.

Several studies have looked at the connection between rock point load index (PLI) and uniaxial compressive strength (UCS) for different rock types. Singh et al. [29] discovered a strong correlation between PLI and UCS across various rock types. The research was important because it helped to

estimate a rock's strength based on PLI, which can be a useful tool for predicting rock properties and optimizing mining operations [29].

Another study by Heidari et al. [9] focused on predicting the compressive and tensile strengths of gypsum rock using point load testing. The authors proposed a method to estimate rock strength from point load tests. The method can be used on various rock types, helping predict rock properties and improving mining operations [28].

Mohamad et al. [20] used particle swarm optimization and backpropagation to predict rock strength. Their method could be combined with existing techniques such as standalone ANN-based PSO and BP models, which could improve the planning and execution of mining activities [20].

Artificial intelligence techniques, including neural networks, fuzzy inference systems, and genetic programming, have improved the accuracy of property predictions made using P-wave velocity, density, and Schmidt hammer rebound numbers [2].

2.4. Application of machine learning in mining operations

Suleymanov et al. [30] developed a machine-learning workflow using artificial neural networks (ANNs) to predict petrophysical properties such as porosity, mineralogy, and pore fluid content from elastic properties. This research showed that ANNs are good for understanding complex rock data.

Machine learning has gained popularity in mining since 2018, with applications covering mineral exploration, extraction, and reclamation phases [14] . These techniques have yielded significant improvements in various aspects of mining operations [2, 26, 34]:

- Optimization of truck dispatch, increasing operational efficiency by 10%
- Potential energy cost reduction of 2.9% in underground mining through machine learning models for refrigeration-ventilation systems
- Equipment performance monitoring and process optimization using unsupervised learning and action learning methods

The implementation of artificial intelligence, machine learning, and autonomous technologies in mining has led to cost savings, increased productivity, and improved worker safety [11].

Inapakurthi [12] demonstrated the use of Recurrent Neural Networks (RNN) with genetic algorithm-tuned hyperparameters to control nonlinear industrial grinding circuits, achieving 97% accuracy.

3. Problem Statement

For operational planning and optimization, it is crucial to predict haulage rates in open pit mining operations. However, this process is complex due to the variability of factors influencing excavation performance, such as rock properties, equipment characteristics, and blasting parameters.

The main problem is the difficulty of integrating these diverse factors into a reliable predictive model. Traditional methods often rely on simplified approximations or operator experience, which can lead to inaccurate estimates and, consequently, no optimal planning of mining operations. Additionally, there is a discrepancy between the theoretical models proposed in academic literature and their practical application in real mining environments. Variability in the properties of the rock at a mining site presents another difficulty. Haulage rate prediction becomes more challenging when the density and strength of the rock fluctuate over shorter distances. Therefore, a mixture of theoretical models and machine learning methods are used in this study to fill in these gaps. Thus, developing a system to predict haulage rates in rock excavation is the purpose of research study.

Developing a system to forecast haulage rates in rock excavation is the goal. This system will employ neural networks to estimate the Al_2O_3 content of rocks to determine their density and point load index. Haulage rates will be calculated by a predictive model using these estimates. As a result, haulage rates can be better predicted, considering changes in rock properties and other operational factors.

4. Research Methodology

Details of the methodology used to implement and evaluate the extraction rate prediction model in mining operations are shown in Figure 1.

Figure 1. Research methodology.

4.1. Data Set

The models were developed and validated using experimental data sets that included values for rock density, Al_2O_3, and $I_s(50)$.

4.2. Data Preprocessing

Before the model was trained, the data was prepared to ensure quality and consistency such that:

- Missing values were handled using imputation techniques.
- Outliers were removed based on the Mahalanobis distance.
- Features were normalized using min-max normalization in TensorFlow.

4.3. Model Design and Training

Two prediction models were developed:

4.3.1. Density Prediction Model

Rock density was estimated based on Al_2O_3 content by this model. A dense neural network with several hidden layers and an output layer was used to predict density.

4.3.2. $I_s(50)$ Prediction Model

$I_s(50)$ is predicted using density and Al_2O_3 content as inputs by this model. The model structure was like the density prediction model.

An example of a neural network is illustrated in Figure 2. This diagram shows the typical structure of an artificial neural network, including input layers, hidden layers, and output layers. The interconnected nodes demonstrate how information flows through the network, with each connection representing a weighted input.

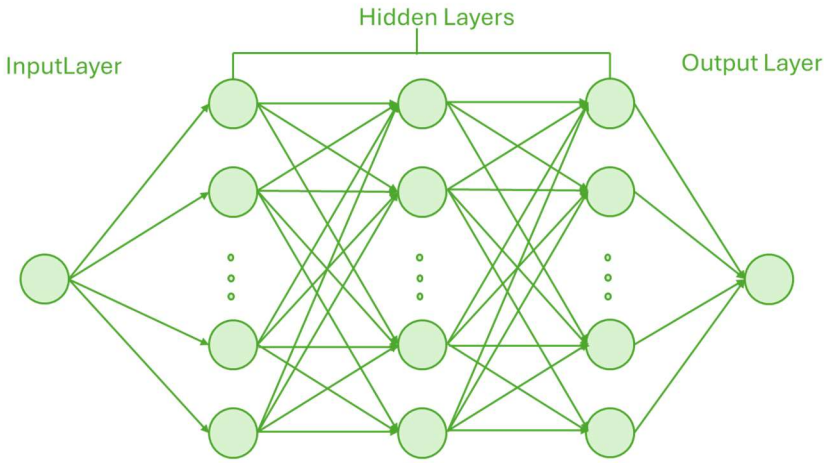

Figure 2. Example neural network.

The models output were used to calculate mucking rates using the production Eq. (1) and Eq. (2) . The extraction rate is calculated by this formula by multiplying an ideal maximum productivity rate by operating efficiency. The efficiency is determined by rock strength (calculated from predicted density and I s (50)), nominal bucket capacity, explosive energy concentration, and three other coefficients.

$$Q = Q^0 e^{-kf_s/B_p}\left[\frac{\sigma^2}{\left(E-E^0\right)^2+\sigma^2}\right] \tag{1}$$

$$f_s = 0.0015p_r - 3 + 0.264I_{s(50)} \tag{2}$$

Where:

Q^0:	Maximum rate
k:	Coefficients in the mathematical mode
f_s:	Rock strength factor
Bp:	Nominal load of the excavator
E:	Powder energy factor
E^0:	Inicial powder energy factor
σ:	Scale factor.
p_r:	Rock density
$I_{s(50)}$:	Point load strength index

The models were trained using training datasets. The mean square error loss function was optimized with the Adam optimizer [36] . Regularization techniques [21] were used in conjunction with hyperparameter tuning to improve model performance.

4.4. Predictive Performance Evaluation

The performance of the model was evaluated using a separate data set. The following metrics were calculated:

- Mean Squared Error (MSE): The average squared difference between predicted and actual values was measured. Lower MSE indicates better model fit.
- Mean Absolute Error (MAE): This measure measures the average absolute difference between predicted values and actual observed values.
- Absolute Percentage Error (MAPE): It measures the average percentage difference between predicted values and actual observed values

Scatter plots and residual plots were also created to visualize the relationship between predicted and actual values and to detect patterns in prediction errors.

4.5. Additional Experiments

More experiments were conducted to explore how different setups affected predictive performance:

- Different model structures were tried, changing the number of hidden layers, neurons per layer, and activation functions.

These results were compared with the initial model and the setup that performed best according to the evaluation metrics was chosen.

5. Case study

The optimal mine design was created using GEOVIA GEMS [31] and further optimized with Minkah [19] . The final design of the pit had a total tonnage of 3,003 Mt, of which 1,566 Mt was ore with grades of 51% Al_2O_3 and 5% SiO_2.

The mine was divided into three pushbacks [3] as presented in Figure 3 for more control and better cash flow. Each pushback has its access ramp. The available material generated by GEOVIA Whittle [32] , the designed pit boundary and pushbacks are presented in Table 1.

Table 1. Summary of material tonnages [10].

Description	Total tonnage (Mt)	Ore tonnage (Mt)
Whittle optimum pit shell	2763.0	1610.0
Designed pit shell	3003.0	1566.0
Pushback 1	822.0	402.0
Pushback 2	1260.0	587.0
Pushback 3	912.0	544.0

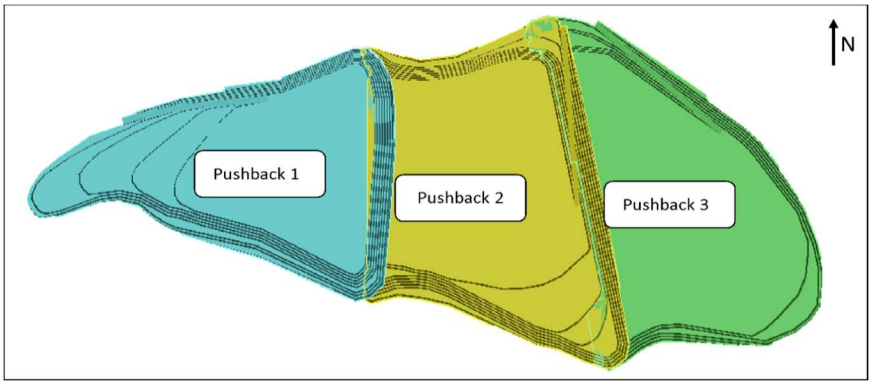

Figure 3. Pushback designs [10].

Economic parameters considered for GEOVIA Whittle [32] to generate the final pit and pushbacks are shown in Table 2.

Table 2. Economic parameters [18].

Description	Value
Reference mining cost	$3.16 /tonne
Reference processing cost	$9.6 /tonne
Reference stockpile cost	$0.5 /tonne
Selling price	$0.76 /%mass
Discount rate	10 %

The design includes a truck transportation system with two loading points and a crushing site. It also includes switchbacks, roads, reclaimers, process plants, tailings, and waste deposits. This conceptual layout is shown in Figure 4.

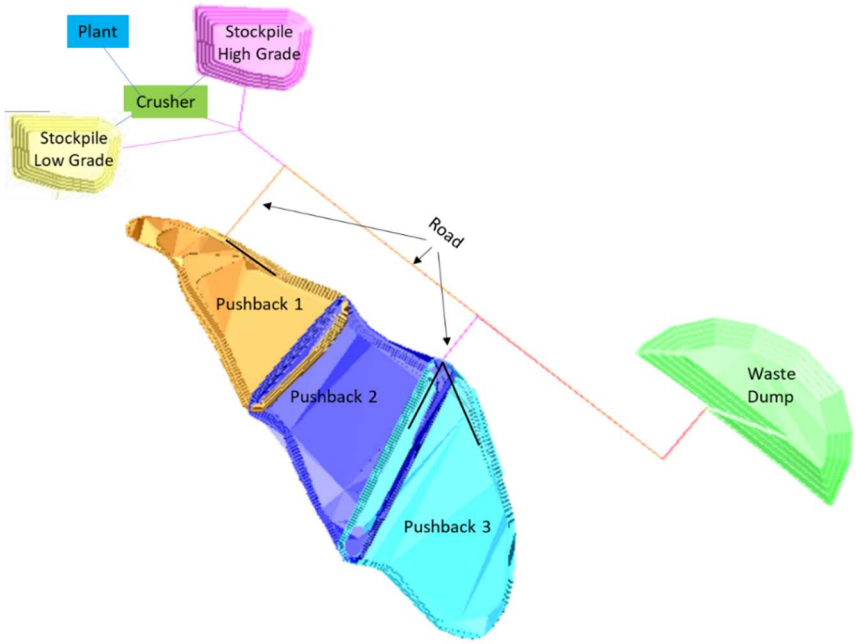

Figure 4. The conceptual design of the operating system [10].

The strategic plan generated in GEOVIA Whittle [33] shows a mine life of 47 years, with a mining rate of 65 Mtpa and processing rates of 25 Mtpa (years 1-19) and 37 Mtpa (year 20 onwards). The mining and processing capacity schedule are presented in Figure 5 and Figure 6 respectively.

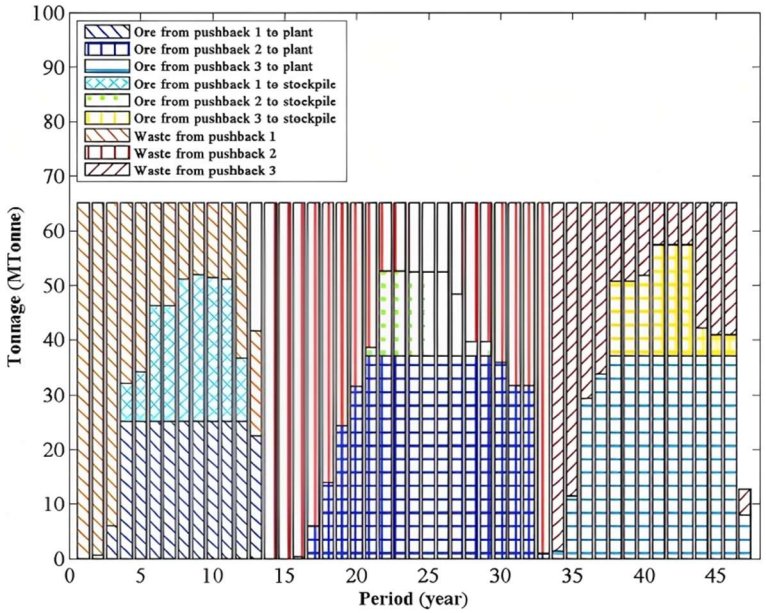

Figure 5. Mining activity in each pushback [10].

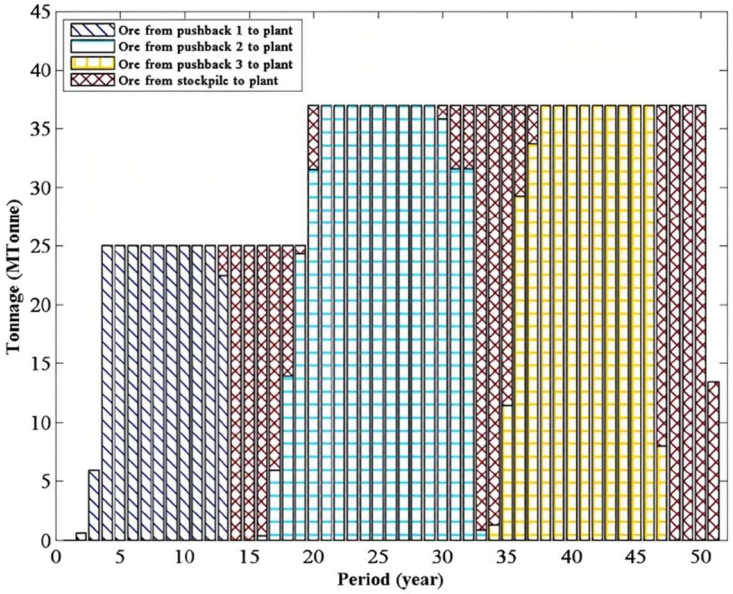

Figure 6. Processing plant material tonnage schedule [10].

A short-term (annual) production schedule was used. The database was extracted from Period 8 of Pushback 1, as this period had a good representation of the material flow of the entire mine.

6. Implementation

Two neural network models were created: one to predict Al_2O_3 content based on density, and the other to estimate $I_s(50)$ using density and Al_2O_3 content. These models were built on TensorFlow and Keras [21] . The results were applied to the production formula to estimate the production ratio of the shovel. In the following subsections, the processes of the model's implementation are explained including development, training, and evaluation.

6.1. Dataset

A database containing information on density, Al_2O_3 content, and Is(50) was required. Information was found in NI 43-101 reports, geological reports, articles, mining magazines, and theses [1, 4, 8, 24, 27]. The database was created with density, Al_2O_3 grade, and $I_s(50)$ as shown in Table 3.

Table 3. Dataset.

Density (kg/m^3)	Al_2O_3 (%)	$I_s(50)$ (Mpa)
3100	85	
1600	55.1	
1790	50.4	
1870	50.9	
2782		1.21
3000		5.36
2800	43.22	
3000	44.78	
1640	51.99	
1880	52.5	
1910	52	
2110	49.1	
2280	53.38	
1980	51.7	
2050	52.03	
2679		4.14
2467		1.39
2778		6.54
3068		4.62
2100		4.97
1850		3.17
1800		2.93
2980	43.623	5.18

6.2. Data Preprocessing

A new database was extracted from the original database. This new database contained only the density and Al_2O_3 values. The data was separated to prepare it for different analyses.

6.3. Neural Network Model for Al2O3 Content Prediction

A neural network model was developed to predict the Al_2O_3 content in a material using its density. A machine learning approach using neural networks was used to find the relationship between these two variables.

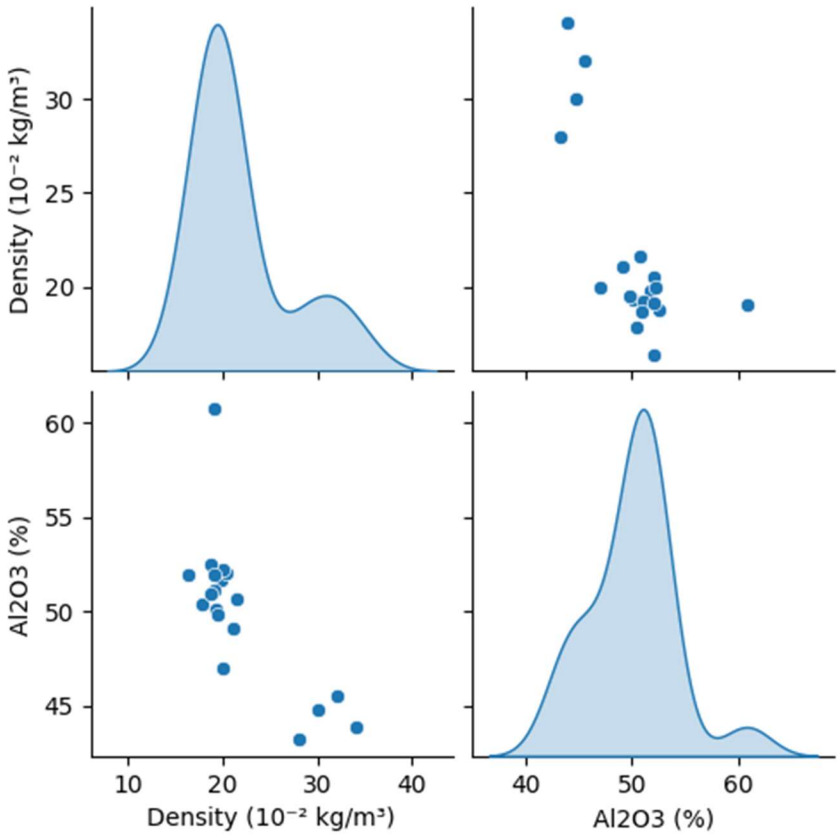

Figure 7. Multivariate Analysis: Density and Al_2O_3 relation.

Figure 7 illustrates the dataset used to train a machine learning model that predicts Al_2O_3content from density. The scatter plot shows the general relationship between these two variables, where higher density tends to be associated with higher Al_2O_3content, although with considerable scatter. The density plots reveal that both the density and Al_2O_3 values follow an approximately normal or bell-shaped distribution.

The algorithm loads a data set containing density and Al_2O_3 content values for different samples. Then, splits the data into training (80%) and test (20%) sets. Before feeding the data to the model, a normalization process was performed. This method scales the input features to a standard range. It helps the model converge faster and perform better. The deep neural network (DNN) model was built using Python's TensorFlow library [23] . The model had four dense layers with 256, 128, 64, and 1 neuron, respectively. The neural network model is defined with several hidden layers and Rectified Linear Unit (ReLU) activation to extract features and learn complex relationships, for the hidden layer.

The input of the model was density, and the output was the Al_2O_3 content. Different layer configurations and numbers of neurons were tested to optimize the model architecture. The goal was to optimize the model architecture to achieve a good fit to the data, without overfitting or underfitting problems. Overfitting occurs when a model learns too much from the training data, capturing noise and performing poorly on new data, while underfitting happens when a model is too simple, failing to capture the underlying patterns in the data [13].

Figure 8 shows how the training loss of the neural network model changes during the training process. The blue line represents the loss on the training data, and the orange line represents the validation loss on the validation data. At the beginning of training, both losses start very high. As the

model learns from the training data, the losses decrease rapidly. The training loss decreases more than the validation loss because the model fits the training data better. After about 4000 epochs (training iterations), the losses stabilize and only decrease slightly. This indicates that the model has learned all it can from the training data and its performance is no longer improving significantly. In general, the validation loss is expected to be low and stable, meaning that the model generalizes well to new data.

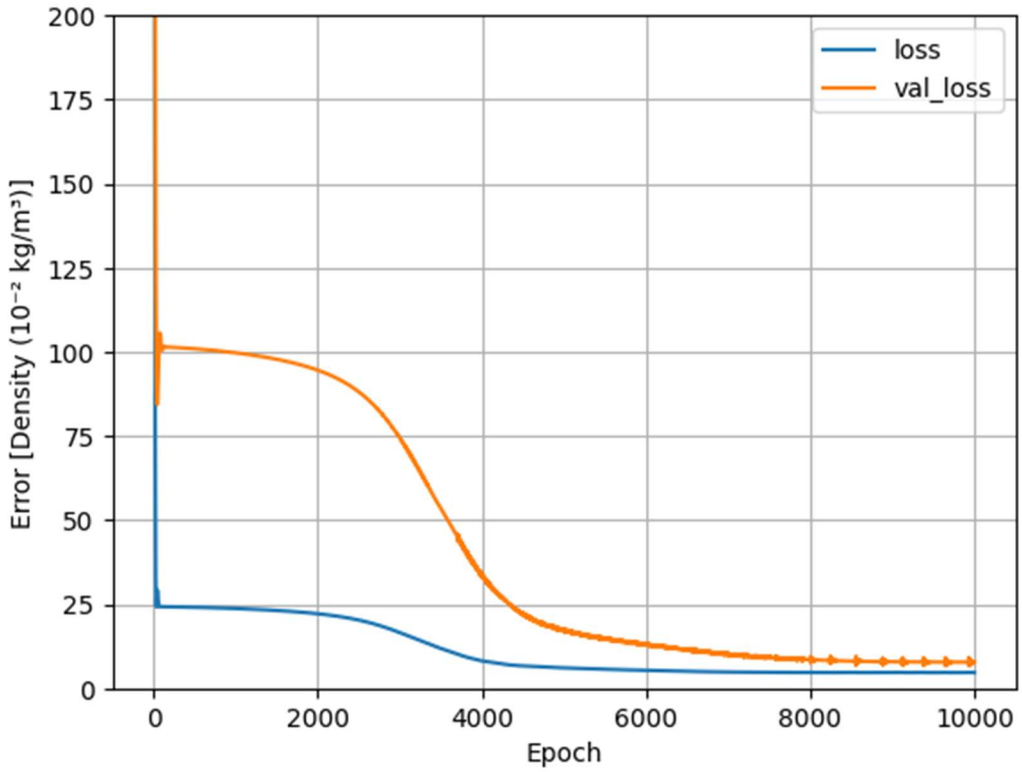

Figure 8. Train and valuation loss during the neural network training process for Al_2O_3.

Figure 9 compares the actual Al_2O_3 values in the data with the predictions made by the neural network model. The horizontal axis represents the Al_2O_3 content, while the vertical axis represents the density. The blue dots show the actual density and Al_2O_3 values in the data. The black line represents the model predictions. For low Al_2O_3 values, the blue dots and the black line coincide almost perfectly, meaning that the model predicts the density values for those Al_2O_3 levels with high accuracy.

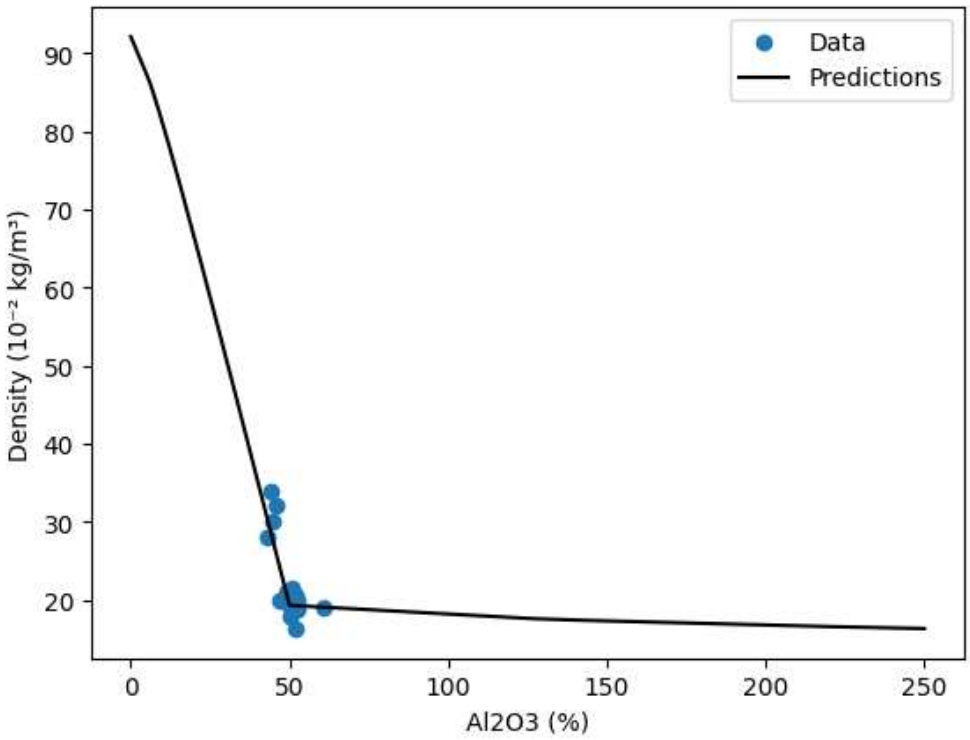

Figure 9. Al_2O_3 vs Density: Model Predictions and Actual Data Comparison.

The model is trained using the Adam optimization algorithm [36] which is used to minimize the loss function during the training of neural networks. During training, the model learns to map the density values to the corresponding Al_2O_3 values. Below are those corresponding to different metrics used to evaluate the performance of a machine learning model.

- Accuracy: The model achieved a Mean Squared Error (MSE) of 11.32, a Mean Absolute Error (MAE) of 2.74, and an Absolute Percentage Error (MAPE) of 13.04. These values present some level of error, but it is an improvement over traditional methods that use linear regression.
- Sensitivity: The model demonstrated higher sensitivity to density values in the medium range (2000-2500 kg/m^3), where most operational decisions are made. This sensitivity allows for more balanced predictions in the density range which is most critical for mining operations.
- Practical improvements: By accurately predicting Al_2O_3 content from density measurements, which are easier and quicker to obtain in the field, this model can significantly speed up the process of ore grade estimation. This can lead to faster decision- making in ore selection and processing.
- Implementation challenges: The main challenge in implementing this model was ensuring consistent and accurate density measurements across the mining operation.

Once the pre-trained model was built, the density was predicted based on Al_2O_3 for a large database. The new database was saved and used later.

6.4. Neural network model for $I_s(50)$ prediction

A neural network model was developed to predict the $I_s(50)$ value for its density and Al_2O_3 content, employing a machine learning approach to find the relationship between these variables. The process began by loading the dataset containing density, Al_2O_3 content, and $I_s(50)$ values. The data was

randomly split into training (80%) and test (20%) sets to ensure impartial evaluation and avoid overfitting.

Figure 10 presents several graphs illustrating the data set used to train and evaluate the machine learning model that predicts the value of $I_s(50)$ from the density and Al_2O_3 content. The dataset is showcased through several graphs, demonstrating that densities, Al_2O_3 amount, and $I_s(50)$ target value follow normal distributions. Although with a significant scatter of points around the linear trend, there is a positive correlation between density and Al_2O_3 content. To better understand the nature of the data and see the relationships the model is trying to record, these pictures are helpful because they show the distributions and relationships between the key variables (density, Al_2O_3 content, and $I_s(50)$) in various formats.

Before using the data in the model, a normalization step was carried out to ensure the input is within a range that improves convergence and predictive performance. This DNN model was built using Python's TensorFlow library and has four hidden layers with 128, 128, 64, and 1 neuron. These parameters allow the model to progressively reduce dimensionality, capturing essential patterns in the data. The layers with ReLU and Sigmoid activations were chosen to balance complexity, prevent vanishing gradients, and support probability estimation. The first three layers use ReLU functions, and the last used Sigmoid function. The model was trained for 10,000 rounds with a batch size of 64. During this, both training loss and validation loss were monitored to assess performance and detect potential overfitting or underfitting.

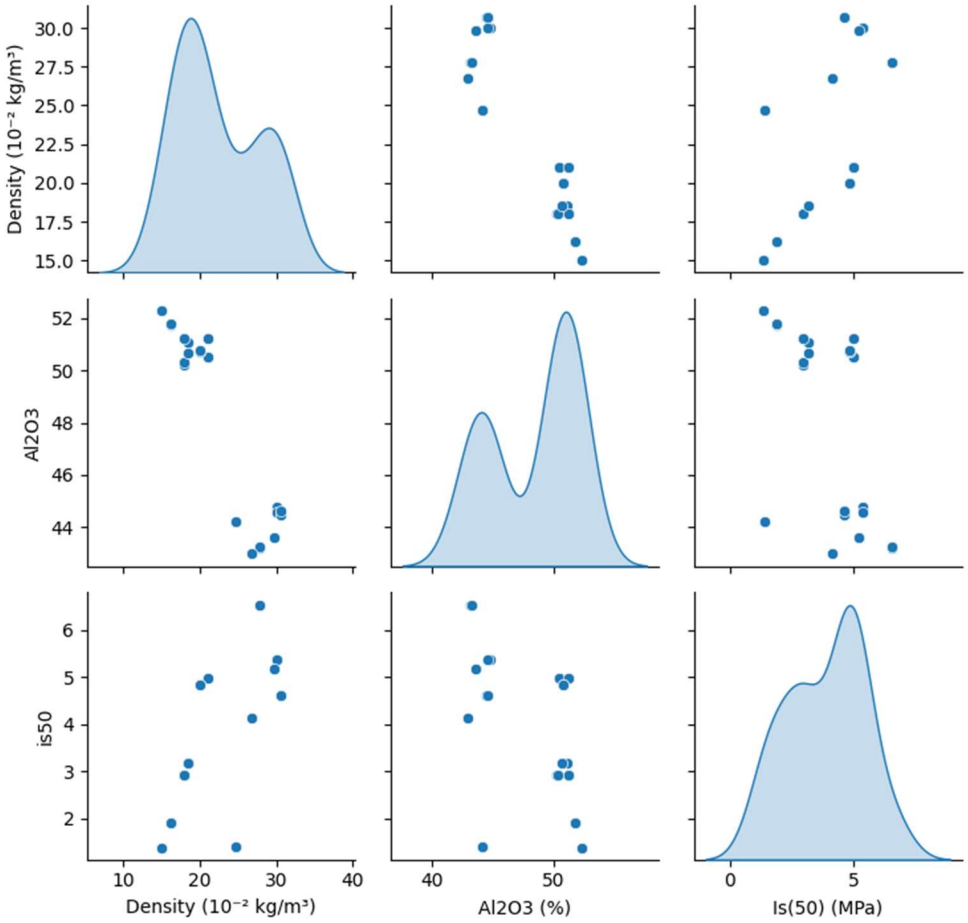

Figure 10. Multivariate Analysis: Density, Al_2O_3, and I_s50 Relationships.

Figure 11 shows the train and valuation loss during the neural network training process for I_s50, with the blue line representing the training data loss, and the orange line showing the validation data loss. Initially, both losses start very high but decrease rapidly as the model learns from the training data, with the training loss decreasing more significantly due to better fit.

After about 4000 epochs (training iterations), the losses stabilize and only decrease slightly. This indicates the model has converged. Once the training process was completed, the performance of the model on the test data set was evaluated.

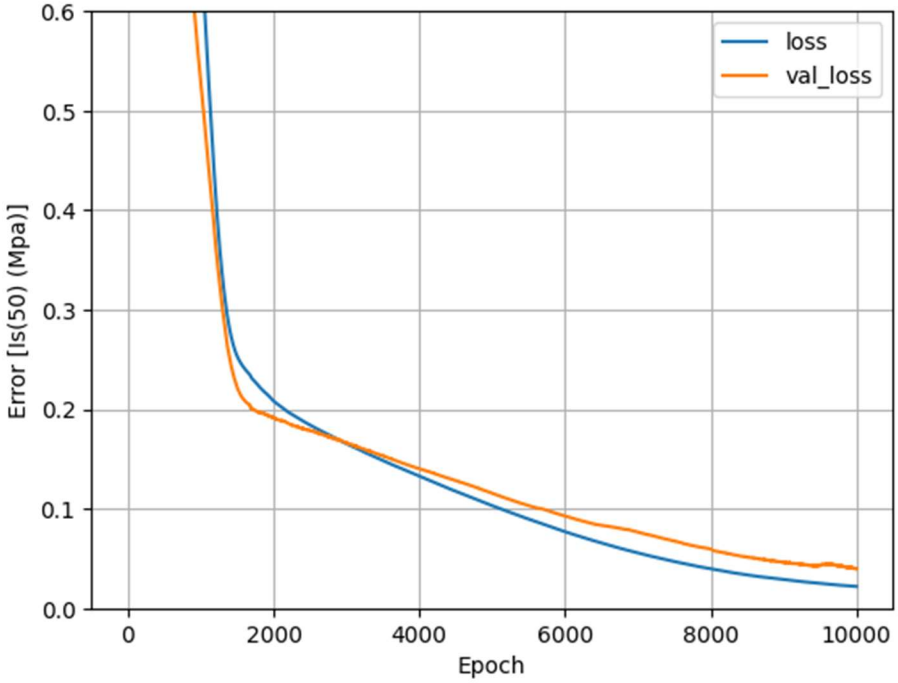

Figure 11. Train and valuation loss during the neural network training process for Is50.

Figure 12 present the predictions of the model vs real values for $I_s(50)$ in the test data set. On the graph, the x-axis shows real values, and the y-axis shows predictions. The diagonal line shows where predictions would match real values perfectly. Each blue dot is a data point from the test set.

Most blue dots are close to the diagonal line, meaning the model's predictions are usually close to the real values. Only one blue dot is a bit far from the line, showing as an outlier.

Overall, this graph shows that the model has excellent predictive performance, with high accuracy in predicting the target property values over almost the entire range of values.

The $I_s(50)$ prediction model, using both density and Al_2O_3 content as inputs, showed exceptional performance:

- Accuracy: With a Mean Squared Error (MSE) of 6.21e-10, Mean Absolute Error (MAE) of 1.87e-05, and Mean Absolute Percentage Error (MAPE) of 1.38e-06, this model demonstrates extremely high accuracy, surpassing traditional empirical methods for estimating rock strength.
- Sensitivity: The model showed high sensitivity to both input parameters, with slightly higher sensitivity to density. This allows for accurate predictions even with small variations in either density or Al_2O_3 content.

- Practical improvements: Accurate $I_s(50)$ predictions can significantly enhance blast design optimization and excavation planning. For example, areas with higher predicted $I_s(50)$ values might require increased explosive charges or different drill patterns.
- Implementation challenges: The accuracy of this model relies on the accuracy of both density and Al_2O_3 content inputs.

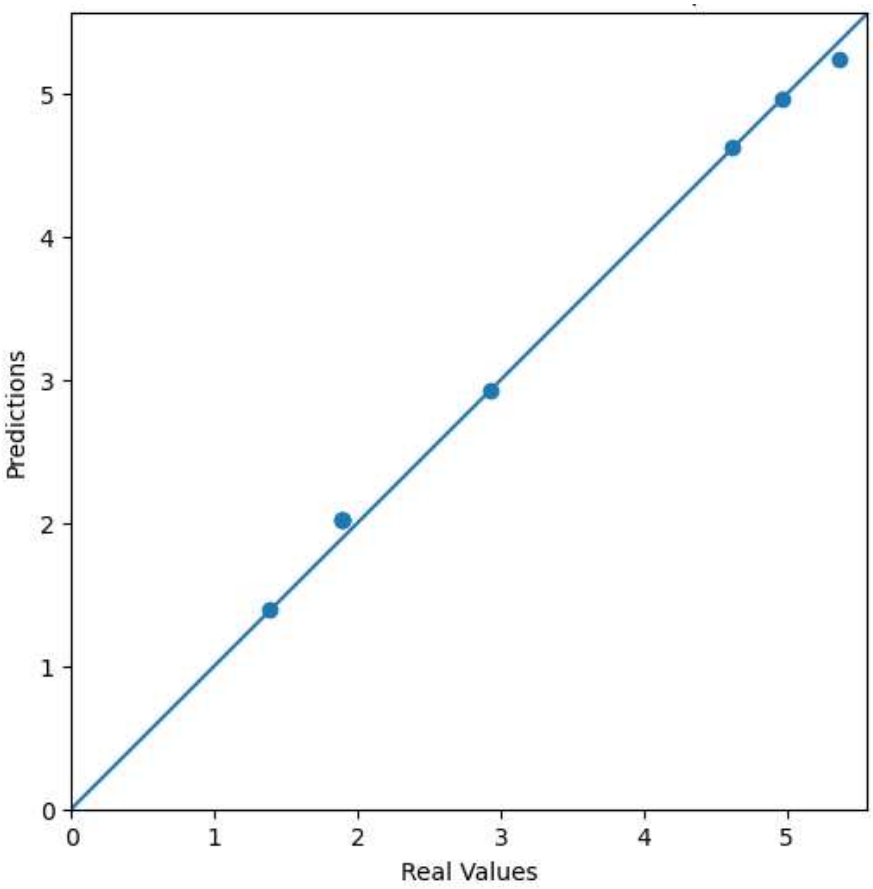

Figure 12. Model Predictions vs Actual Values.

6.5. Production Rate Estimation

Once the pre-trained model is built, $I_s(50)$ is predicted for a large database. The new database is saved with the predictions to be applied in Eq (1).

To apply the model, the predicted values were used in the production formula to estimate shovel rates. In the implementation, the following parameters were used:

- BP (nominal load of the excavator): 80 tons
- Maximum rate of the ideal shovel: 2455 ton/h
- Coefficient k: 12.4 tons
- E (powder energy factor): assumed to be equal to E0 (optimal energy concentration)

Other parameters were kept constant for this experiment. This approach allows us to estimate how changes in rock properties (as predicted by the model) might affect shovel productivity in a mining operation.

Figure 13 presents the relationship between material density and the production rate of the excavator shovel. A clear trend was observed: as the density of the material increases, the production ratio of the blade decreases significantly. The production rate showed an inverse relationship with material density, peaking at medium-low densities (2000-2200 kg/m³) before declining sharply and stabilizing at higher densities.

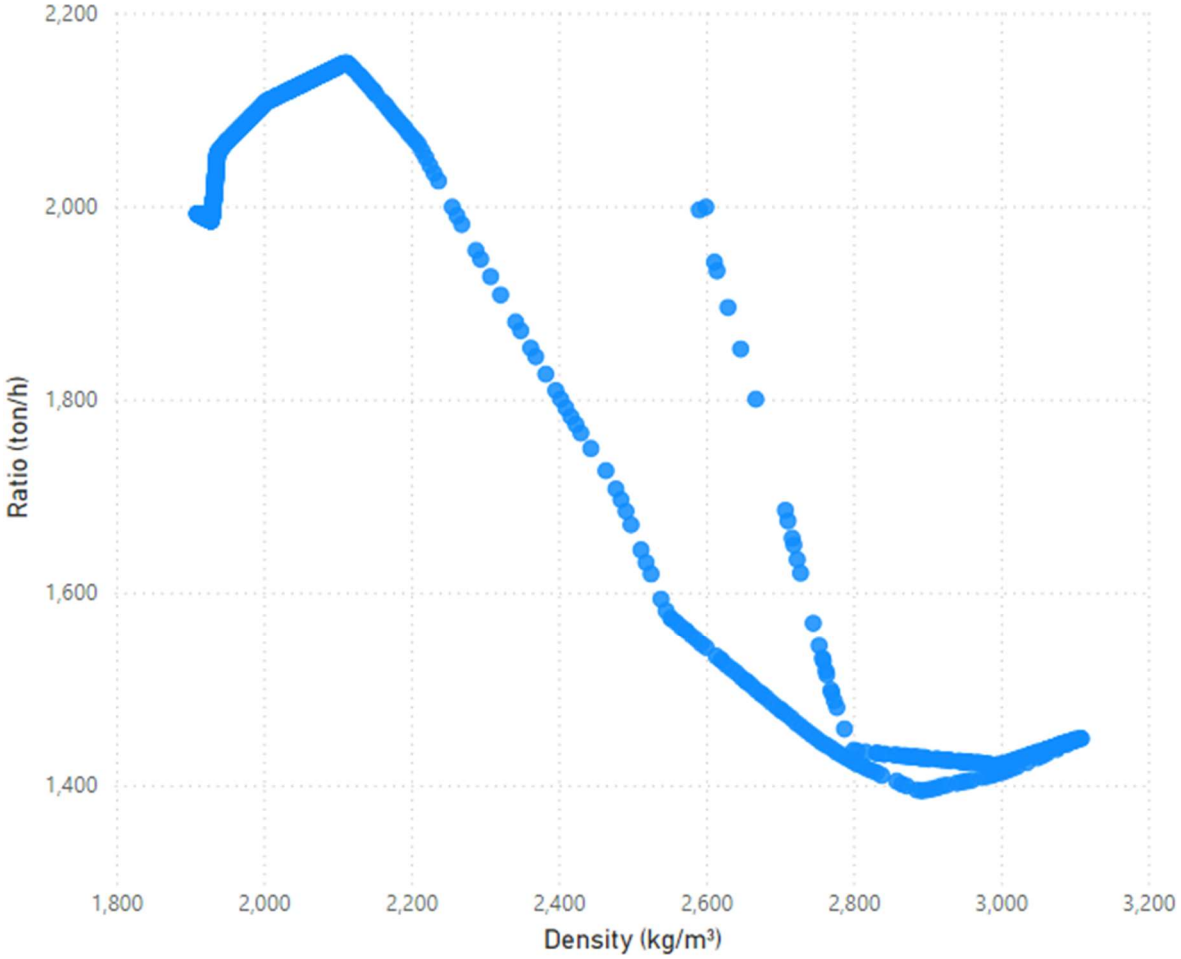

Figure 13. Relation Ratio and Density.

The shovel production ratio location in the selected mining area is presented in Figure 14. It is observed variability in productivity across the pit. It allows the identification of areas with high and low efficiency, which can influence decisions on excavation routes, extraction sequence, and the possible need for specialized techniques or equipment in specific areas. After integrating the predictions from both models into the production rate formula, we observed significant insights were observed:

- The relationship shows that in areas with denser material lower production rates should be expected, resulting in additional digging time and potentially higher fuel consumption and operating costs.
- The production ratio map revealed variability in productivity across the pit, with higher ratios on the center-left portion. This spatial variation in productivity could significantly influence decision-making in mine planning and operations.

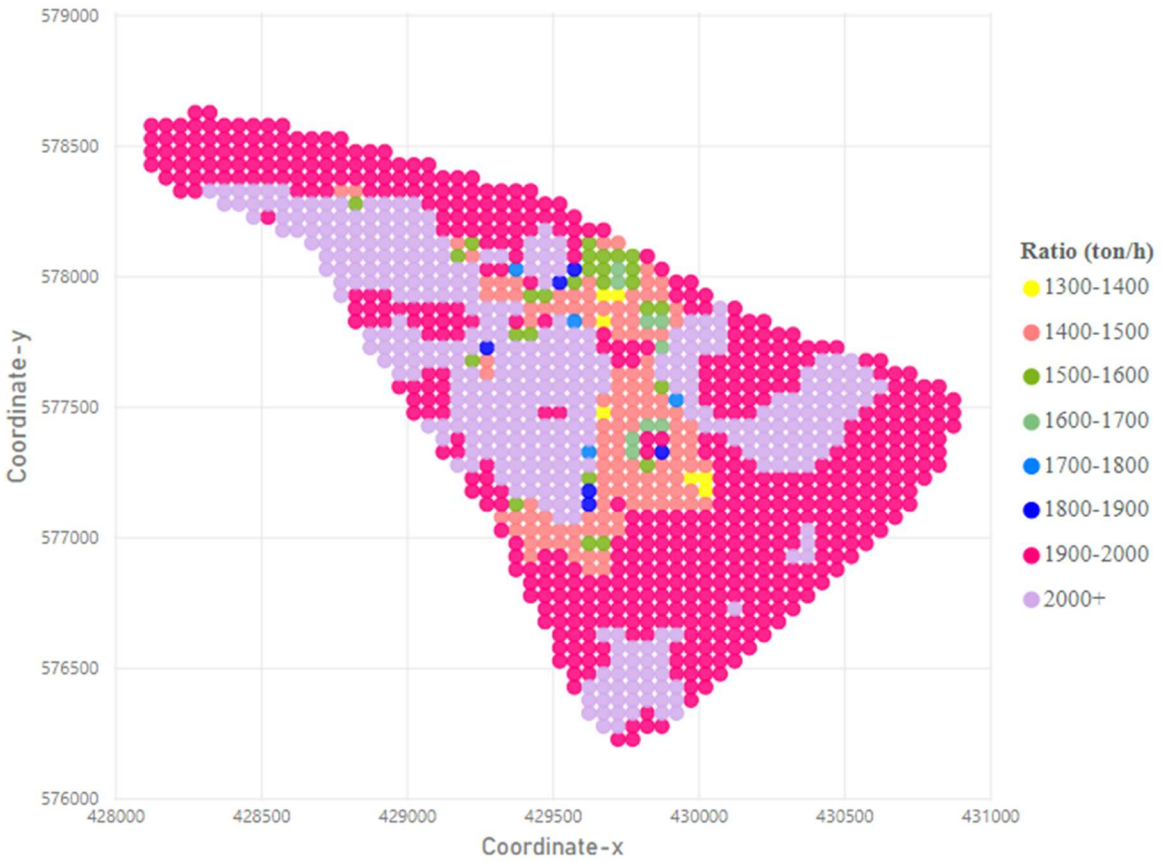

Figure 14. Production Ratio Map.

7. Practical Implications for Mining Operations

These predictive models and their integration into production rate estimation offer several practical benefits for mining operations:

- Improved planning: Mine planners can use these predictions to optimize extraction sequences, prioritizing areas with favorable density and strength characteristics to maximize productivity.
- Equipment allocation: Understanding the spatial variation in production rates can inform decisions on equipment allocation. For instance, more powerful excavators might be assigned to areas with higher predicted $I_s(50)$ values.
- Blast design optimization: Areas with higher predicted $I_s(50)$ values may require adjusted blast designs to ensure optimal fragmentation, potentially saving on explosive costs in areas with lower strength predictions.
- Operational forecasting: More accurate predictions of production rates can lead to improved short-term and long-term production forecasts, enhancing overall mine planning and scheduling.
- Cost estimation: By better understanding relationships between the geology and production rates, excavation operations can be cost-estimated more accurately, improving financial planning.

8. Conclusion

A new approach to predicting production rates in rock excavation operations was developed to forecast shovel production rates in a bauxite mine. Two neural network models were developed: one to estimate rock density from the Al_2O_3 content, and another to predict the $I_s(50)$ using density and Al_2O_3 content as inputs. Rock density and strength predictions were incorporated into a production model to calculate mucking rates.

Deep learning techniques were employed to predict production rates considering the properties of the rock in the deposit. Excavation plans and operations can optimize and maximize the efficiency and utilization of your resources by incorporating predictions of rock characteristics.

This research has the potential of improving mining efficiency and sustainability, using production rate predictions that would manage to more optimal resource allocation, reduce energy consumption, and minimize negative environmental impacts.

This research shows how machine learning combined with traditional mining models can make mines more adaptive and data-driven. Despite further validation may be needed, the study has demonstrated the promising potential of the proposed approach in improving open pit mining operations.

9. References

[1] Abzalov, M., *Bauxite deposits.* Applied Mining Geology, 2016. **12**, pp. 411-425.

[2] Ali, M., and S.H., Lai, *Artificial intelligent techniques for prediction of rock strength and deformation properties – A review.* Structures, 2023. **55**, pp. 1542-1555.

[3] Ben-Awuah, E. and N.S., Hosseini, *An economic evaluation of a primary haulage system for a Bauxite mine: load and haul versus in-pit crushing and conveying.* MOL Report Eight, 2017.

[4] Butty, D. L., G., Wiatzka, P. R., Bedell, R., Gagnon, N., Menard, R., Marchand, D.M., Gagnon, and D., Houde, *NI 43-101 technical report: Bankable feasibility study update of the Bonasika project, Guyana*. First Bauxite Corporation, 2011.

[5] Cao, H., G., Ma, P., Liu, X., Qin, C., Wu, and J., Lu, *Multi-factor analysis on the stability of high slopes in open-pit mines.* Applied Sciences, 2023. **13**(10), p. 5940.

[6] Erarslan, K., and N., Celebi, *A simulative model for optimum open pit design.* CIM bulletin, 2001. **94**(1055), pp. 59-68.

[7] Fytas, K., J., Hadjigeorgiou, and J., Collins, *Production scheduling optimization in open pit mines.* International Journal of Surface Mining and Reclamation, 1993. **7**, pp. 1-9.

[8] Gallo, E.A., *Summary report: Ganhdhamardan bauxite deposit, Sambalpur and Balangir Districts.* Balaton Power Inc., 2007.

[9] Heidari, M., G., Khanlari, M., Torabi Kaveh, and S., Kargarian, *Predicting the uniaxial compressive and tensile strengths of gypsum rock by point load testing.* Rock Mechanics and Rock Engineering, 2012. **45**, pp. 265-273.

[10] Ben-Awuah, E., and N.S., Hosseini, *An economic evaluation of a primary haulage system for a bauxite mine: Load and haul versus in-pit crushing and conveying.* MOL Report Eight, 2017.

[11] Hyder, Z., K., Siau, and F., Nah, *Artificial intelligence, machine learning, and autonomous technologies in mining industry.* Journal of Database Management (JDM), 2019. **30**(2), pp. 67-79.

[12] Inapakurthi, R.K., S.S., Miriyala, and K., Mitra, *Recurrent neural networks based modelling of industrial grinding operation.* Chemical Engineering Science, 2020. **219,** p. 115585.

[13] Inc, S.D., *Overfitting and underfitting in ML: Introduction, techniques, and future.* ScribbleData, 2024.

[14] Jung, D., and Y., Choi, *Systematic review of machine learning applications in mining: Exploration, exploitation, and reclamation.* Minerals, 2021. **11**(2), p. 148.

[15] Khodayari, A., and A., Jafarnejad, *Cut-off grade optimization for maximizing the output rate.* International Journal of Mining and Geo-Engineering, 2012. **46**(2), pp. 157-162.

[16] Kolapo, P., G.O., Oniyide, K.O., Said, A.I., Lawal, M., Onifade, and P., Munemo, *An overview of slope failure in mining operations.* Mining, 2022. **2**(2), pp. 350-384.

[17] Lisboa, A.C., F.H., De Souza, C.M., Ribeiro, C.A., Maia, R.R., Saldanha, F.L., Castro, and D.A., Vieira, *On modelling and simulating open pit mine through stochastic timed petri nets.* IEEE Access, 2019. **7**, pp. 112821-112835.

[18] Lukashuk, O., K., Letnev, and V., Makarova, *Modeling the process of rock excavation with a front-shovel operational equipment of open-pit excavators*, in *Proceedings of Proceedings of the 7th International Conference on Industrial Engineering (ICIE 2021)*. 2022. pp. 425-433.

[19] Minkah, E.A., *Determination of optimized Inchiniso pit, Ghana Bauxite Company Limited.* Thesis, 2014. University of Mines and Technology, Tarkwa. p. 86.

[20] Mohamad, E.T., D.J., Armaghani, E., Momeni, A.H., Yazdavar, and M., Ebrahimi, *Rock strength estimation: A PSO-based BP approach.* Neural Computing and Applications, 2018. **30,** pp. 1635-1646.

[21] Nursat, I., and S.B., Jang, *A comparison of regularization techniques in deep neural networks*. Symmetry, 2018. **10**(11), p. 648.

[22] Ozdemir, B., and M., Kumral, *Appraising production targets through agent-based Petri net simulation of material handling systems in open pit mines.* Simulation Modelling Practice and Theory, 2018, **87,** pp. 138-154.

[23] Pang, B., E., Nijkamp, and Y.N., Wu, *Deep learning with tensorflow: A review.* Journal of Educational and Behavioral Statistics, 2020.**45**(2), pp. 227-248.

[24] Patterson, S.H., *Bauxite reserves and potential aluminum resources of the world*. U. 1967.

[25] Ramazan, S., and R., Dimitrakopoulos, *Recent applications of operations research and efficient MIP formulations in open pit mining.* SME Transactions, 2004. **316**, pp. 73-78.

[26] Ristovski, K., C., Gupta, K., Harada, and H.K., Tang, *Dispatch with confidence: Integration of machine learning, optimization and simulation for open pit mines*, in *Proceedings of Proceedings of the 23rd ACM SIGKDD International Conference on Knowledge Discovery and Data Mining.* 2017. pp. 1981-1989.

[27] Sahu, R.K., *Application of ripper-dozer combination in surface mines: its applicability and performance study.* Thesis, 2012. National Institute of Technology, India.

[28] Segarra, P., J., Sanchidrián, L., López, and E., Querol, *On the prediction of mucking rates in metal ore blasting.* Journal of Mining Science, 2010. **46,** pp. 167-176.

[29] Singh, T.N., A., Kainthola, and A., Venkatesh, *Correlation between point load index and uniaxial compressive strength for different rock types.* Rock Mechanics and Rock Engineering, 2012. **45**, pp. 259-264.

[30] Suleymanov, V., A., El-Husseiny, and J., Dvorkin, *Petrophysical rock properties prediction from elastic properties using artificial neural network (ANN)*, in Proceedings of Sixth EAGE Rock Physics Workshop. 2022. pp. 1-5.

[31] Systèmes, D., Geovia GEMS: Strategic mine planning software, Ver. 6.8.3. 2019.

[32] Systèmes, D. (2019). Geovia Whittle: Strategic mine planning software, Ver. 4.7.3. 2019.

[33] Systèmes, D. (2019). Whittle. Strategic mine planning software. Ver. 4.7.3, Vancouver.

[34] Zelinska, S., *Machine learning: technologies and potential application at mining companies,* in *Proceedings of The International Conference on Sustainable Futures: Environmental, Technological, Social and Economic Matters (ICSF 2020).* 2020. pp. 5.

[35] Zhang, K., J., Zuo, and Y., Zhai, *Analysis of the advantages of open pit mining.* Scientific Journal of Technology, 2024. **6**(3), pp. 95-98.

[36] Zhang, Z., *Improved adam optimizer for deep neural networks,* in *Proceedings of 2018 IEEE/ACM 26th international symposium on quality of service (IWQoS), IEEE.* 2018. pp.1-2.